Environmental Science & Technology

pubs.acs.org/est

Article

Low-Level Cefepime Exposure Induces High-Level Resistance in Environmental Bacteria: Molecular Mechanism and Evolutionary Dynamics

Hanqing Wang, Youjun Feng,* and Huijie Lu*

Cite This: *Environ. Sci. Technol.* 2022, 56, 15074−15083

Read Online

ACCESS | Metrics & More | Article Recommendations | Supporting Information

ABSTRACT: Antibiotics exert selective pressures on clinically relevant antibiotic resistance. It is critical to understand how antibiotic resistance evolves in environmental microbes exposed to subinhibitory concentrations of antibiotics and whether evolutionary dynamics and emergence of resistance are predictable. In this study, *Comamonas testosteroni* isolated from wastewater activated sludge were subcultured in a medium containing 10 ng/mL cefepime for 40 days (~300 generations). Stepwise mutations were accumulated, leading to an ultimate 200-fold increase in the minimum inhibitory concentration (MIC) of cefepime. Early stage mutation in DNA polymerase-encoding gene *dnaE2* played an important role in antibiotic resistance evolution. Diverse resistance mechanisms were employed and validated experimentally, including increased efflux, biofilm formation, reduced antibiotic uptake, and drug inactivation. The cefepime minimal selective concentrations (MSCs) and relative fitness of susceptible, intermediate, and resistant mutants were determined. Agent-based modeling of the modified Moran process enabled simulations of resistance evolution and predictions of the emergence time and frequency of resistant mutants. The unraveled cefepime resistance mechanisms could be employed by broader bacteria, and the newly developed model is applicable to the predictions of general resistance evolution. The improved knowledge facilitates the assessment, prediction, and mitigation of antibiotic resistance progression in antibiotic-polluted environments.

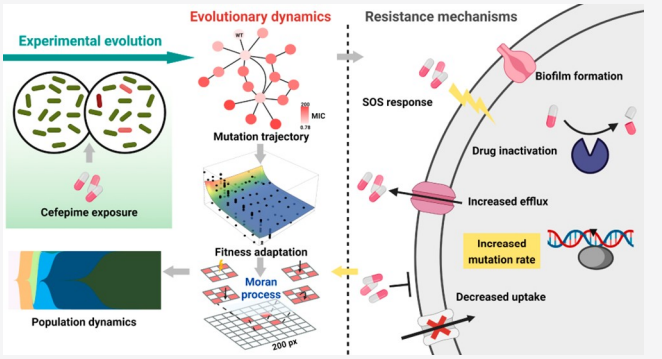

KEYWORDS: *antibiotic resistance, evolutionary dynamics, fitness landscape, agent-based modeling, modified Moran process*

1. INTRODUCTION

Antibiotic resistance represents an essential "One Health" issue and has been extensively studied for decades at clinically relevant concentrations.[1] Antibiotic concentrations in water, soil, and sediment are normally lower than their minimum inhibitory concentrations (MICs), but up to several hundred-fold increases in antibiotic resistance can be developed by stepwise selections of successive mutations[2] and the enrichment of pre-existing resistant mutants in the population.[3] This process has been significantly accelerated by the overuse of antibiotics, placing a few of them in the European Commission Surface Water Watch List, e.g., ciprofloxacin and amoxicillin.[4] Therefore, one of the challenging tasks of combating antimicrobial resistance (AMR) is to reduce the rate at which antibiotic resistant bacteria (ARB) and antibiotic resistance genes (ARGs) evolve in the environment.[5]

Bacteria develop AMR through varied mechanisms, e.g., increased expression of efflux pumps and decreased antibiotic uptake, which often involve spontaneous mutations.[6,7] Under mild antibiotic selection in the environment, diversified mutations conferring resistance are expected. For example, Santos-Lopez et al. found that exposure to sub-MICs of ciprofloxacin resulted in the development of unique drug resistance mutations involving elevated multidrug efflux and horizontal gene transfer, which were absent in cultures exposed to concentrations of ciprofloxacin above its MIC.[8] Stepwise evolution from low-level resistance allows epistatic interactions between multiple genes and reduces the fitness cost arising from resistance mutations.[9] Intriguingly, a few highly resistant mutants can contribute to the strong phenotypic resistance of a population or community. Xing et al. suggested that strongly resistant mutants representing only 10^{-5} of the population can significantly increase streptomycin resistance.[10] How environmental level antibiotics select diversified mutations and whether the evolution of antibiotic resistance can be predicted

Special Issue: Antimicrobial Resistance in the Environment: Informing Policy and Practice to Prevent the Spread

Received: January 30, 2022
Revised: May 5, 2022
Accepted: May 10, 2022
Published: May 24, 2022

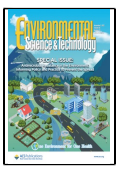

https://doi.org/10.1021/acs.est.2c00793
Environ. Sci. Technol. 2022, 56, 15074−15083

are key questions to be addressed for mitigating ARB/ARG transmissions from the environment to humans.

Comamonas testosteroni (formally *Pseudomonas testosteroni*) are aerobic, Gram-negative bacteria ubiquitously distributed in soil, surface water, and ocean sediments. *Comamonas* species are environmentally important due to their diversified niches. A carried larger genome (~6 Mb) suggests that the genus *Comamonas* represents a group of bacteria that can adapt very well, both ecologically and physiologically, to environments.[11] They occasionally cause human infections and confer broad-spectrum antimicrobial resistance due to the acquisition of the plasmid-mediated blaNDM1 gene.[12,13] Cefepime is a fourth-generation cephalosporin (CEPH) with broad-spectrum antimicrobial activity and a MIC value of around 1 μg/mL.[14] It can irreversibly inhibit the cross-linking between penicillin-binding proteins (PBPs) and peptidoglycan to disrupt cell wall synthesis.[15] Clinical resistance to cefepime is often mediated by mutations of β-lactamase responsible for drug hydrolysis, e.g., Bla, TEM, and CTX.[16,17] Due to being broadly prescribed and having low biodegradability, cefepime and other CEPHs have been detected at increasing concentrations in surface water (0.08−1.12 ng/mL), treated domestic wastewater (2.9−64 ng/mL), and treated hospital sewage (2.38−540.89 ng/mL).[18]

In this study, we aimed to reveal the molecular mechanism and evolutionary dynamics of antibiotic resistance in environmental bacteria exposed to subinhibitory levels of cefepime and develop an evolutionary dynamics model on the basis of the fitness landscape of mutated genotypes. Experimental evolution was performed using *Comamonas testosteroni* isolated from wastewater activated sludge as a representative environmental microbe and at a representative environmental concentration of cefepime (10 ng/mL). Thereafter, growth-competition experiments were conducted between harvested mutant strains and the wild-type strain at varied cefepime concentrations (0.04−160 ng/mL) to estimate their relative fitness (Figure S1). The evolutionary trajectories were reconstructed to infer the molecular mechanism of cefepime resistance. A generalized, agent-based model was developed for the simulation of evolutionary dynamics on the basis of the modified Moran process and the prediction of the emergence of high-level resistance under environmental-level antibiotic selection pressures.

2. MATERIALS AND METHODS

2.1. Bacterial Strain, Media, and Antibiotic. The *C. testosteroni* ancestor strain was isolated from the aeration tank in a municipal wastewater treatment plant (Figure S2) and cultured in LB medium. The MIC measurement experiment was conducted in a CAMHB medium (CBMORE). Cefepime (>98%, Macklin) was dissolved in 0.1 M, pH 6.0 phosphate buffered saline (PBS) as the antibiotic stock solution.

2.2. Experimental Evolution. The *C. testosteroni* ancestor strain was preadapted prior to experimental evolution. A single colony was picked from the agar plate and grown in 5 mL of LB medium at 30 °C and 150 rpm for 24 h. Subsequently, the suspension was 1:100 diluted into a new shake tube, and the process was repeated for 10 days (~6.64 generations per day). At the end of the preadaptation phase, a single clone of *C. testosteroni* X13 (GenBank accession number CP090445) was selected as the wild-type (WT) strain and grown overnight in LB medium. Afterward, triplicate lineages were subcultured on a daily basis in LB medium with 10 ng/mL cefepime for 40 days. Three control lineages were cultured under the same condition without cefepime. Experimental evolution was conducted in Abgene 96-well, 2.2 mL polypropylene deep well storage plates (Thermo Scientific, #AB0661) sealed with breathable sealing film (Corning, #1223S04). Subcultures collected on days 4, 8, 12, 16, 20, 24, 28, 32, 36, and 40 were frozen in 30% glycerol at −80 °C. The optical density (OD) at 600 nm was measured for all cultures, and no growth was observed in the blank control.

To determine the frequencies of the resistant cells in the population (i.e., frequency of resistance), populations collected on days 4, 12, 20, 28, 36, and 40 were serially diluted and spread on LB agar plates with cefepime at 0, 2, 10, and 100 μg/mL. The frequency of resistance was calculated as the number of colonies formed on plates with cefepime (unit: CFU per mL) relative to the total number of colonies grown on antibiotic-free plates (unit: CFU per mL).

To reconstruct the evolutionary trajectory of antibiotic resistance, we selected *C. testosteroni* mutants with increasing resistance to cefepime by plating cultures of a randomly revived lineage on LB agar plates containing cefepime at 1× or 0.5× of the population MIC. Three clones were randomly picked from each plate after 24 h of incubation at 30 °C and reisolated on plates with the same concentration of cefepime. Subsequently, 60 strains at the 10 evolution nodes were tested for genetic stability. Among them, 57 strains maintained the same MIC values of cefepime after 3 days of passaging without cefepime (~20 generations) and were used for resequencing.

2.3. Phenotypic Characterization. The phenotypic characterization of selected resistant mutants included bacterial growth curve measurements, MIC measurements by microbroth dilution, the biofilm formation assay by crystal violet staining, reactive oxygen species (ROS) measurements by the DCFDA method, and outer membrane (OM) permeability measurements by the *N*-phenyl-1-naphthylamine (NPN) uptake assay according to standard methods. More experimental details can be found in the Supporting Information Methods Section.

2.4. Whole-Genome Sequencing and Resequencing. The WT strain was sequenced using PacBio RS combined with Illumina sequencing (NovaSeq6000). The Illumina data were used to evaluate the complexity of the genome and correct the PacBio long reads. The high-quality assembled genome of the WT strain (total length = 5 894 614 bp, complete) served as the reference genome for variant detection (Figure S3). 57 selected variants (see Section 2.2) were resequenced on the Illumina platform. Single nucleotide polymorphisms (SNPs), small indels, and structural variants were identified on the basis of the resequencing data. Experimental details of gDNA extraction, quality control, sequencing, and bioinformatic analysis can be found in the Supporting Information Methods Section.

2.5. Mutation Rate Estimation. The mutation rates of the WT strain and *dnaE2* mutant were estimated by fluctuation tests.[19] As described previously,[20] the strains were revived from the −80 °C stock grown overnight in 100 μL of LB medium without cefepime. Strains were subject to $1/10^7$ dilution to remove any pre-existing mutations. 80 independent subcultures per strain were established in 1 mL of LB medium, and ten were randomly picked to estimate the population size by plating. Cefepime-resistant subcultures were detected by plating a fraction of each culture on LB agar medium

https://doi.org/10.1021/acs.est.2c00793
Environ. Sci. Technol. 2022, 56, 15074−15083

containing 100 μg/mL cefepime. Colonies were counted following the drop plate method.[21] The mutation rate was estimated by performing the Luria−Delbrück fluctuation analysis using the Fluctuation AnaLysis CalculatOR (FALCOR) tool.[22]

2.6. RT-qPCR Assay. Triplicate cultures were collected after a 3 h exposure to 1 μg/mL cefepime for RNA extraction using the RNeasy mini kit (Qiagen, USA). The removal of genomic DNA and reverse transcription reaction for cDNA synthesis were performed using the PrimeScript RT reagent kit (Takara Bio, Japan). Quantitative PCR was then carried out to quantify the expression levels of the target genes (*gyrB*, *oprN*, *mexJ*, *yoeA*, and *emrA*) using the CFX Connect Real-Time PCR detection system (Bio-Rad, USA). Specific PCR primers were designed on the basis of the genome sequence of the WT strain (Table S1). The qPCR conditions were 95 °C for 3 min, followed by 40 cycles of 95 °C for 30 s, a specific melting temperature for 30 s, and 72 °C for 30 s. The amplification efficiency varied between 95% and 105%. The transcripts of the target genes were normalized by *gyrB* transcripts to calculate the relative gene expression levels (Livak method).

2.7. Measurement of Cefepime and Identification of Degradation Products. The cefepime concentration was measured by UPLC-MS/MS (Xevo TQ-S, Waters, USA). The Waters BEH HILIC column (100 mm × 2.1 mm, 130 Å, 1.7 μm) was used for the separation of analytes. UPLC-Q-TOF-MS (AB SCIEX, CA, USA) and SCIEX OS Software 2.1.6 (AB SCIEX, CA, USA) were used to identify the degradation products of cefepime. More experimental details of UPLC-MS/MS and UPLC-Q-TOF-MS can be found in the Supporting Information Methods Section.

2.8. Relative Fitness Prediction. To predict the relative fitness (w) of specific mutant genotypes in a high-throughput manner, we followed a previously described approach based on monoculture and mixed-culture growth curves.[23] Briefly, the growth curves of the WT strain and mutants were measured in monoculture and 50:50 mixed culture with cefepime in a 4-fold dilution series (0.04−160 ng/mL). The *Curveball* package (https://curveball.yoavram.com) was used to analyze the growth data and calculate the relative fitness of all mutants (w_0 of the WT strain was set as 1).

2.9. Agent-Based Modeling of Evolutionary Dynamics. Seventeen genotypes (1 WT and 16 mutants) and their evolutionary relationships were built in an undirected graph. The undirected graph was stored in an adjacency matrix, and the calculated relative fitness (or reproduction rate) of all the genotypes was stored in a database. Population dynamics simulation was carried out on a two-dimensional 200 × 200 chessboard. Each cell was modeled as a grid of unit length. The dynamics of mutation−selection and birth−death processes were simulated on the basis of a modified Moran model.[24] In brief, (i) the initial population size N was set as 40 000, consisting of only WT; (ii) at each step, individual cells had the same probability (μ, mutation rate) to jump from the current genotype to the adjacent genotype; (iii) a number of individuals (n) were chosen for reproduction with a probability proportional to their relative fitness (the static fitness of an individual was determined by its genotype in the absence of cell−cell interactions). Meanwhile, the same number of individuals was eliminated. (iv) The eliminated individuals were replaced by reproductive offsprings. The output data included all mutation events that occurred during simulated evolution and the dynamics of all genotypes. The modeling program was written in Java, and simulations were performed in Anylogic (v 8.5.2).

3. RESULTS AND DISCUSSION

3.1. Antibiotic Resistance Evolved during Exposure to an Environmental Level of Cefepime. The isogenic wild-type strains of *C. testosteroni* were stressed by cefepime at 10 ng/mL for 40 days. The population MIC increased rapidly from 0.78 μg/mL to a maximum of 200 μg/mL, reaching a plateau around day 28 (Figure 1A), and the pattern was similar

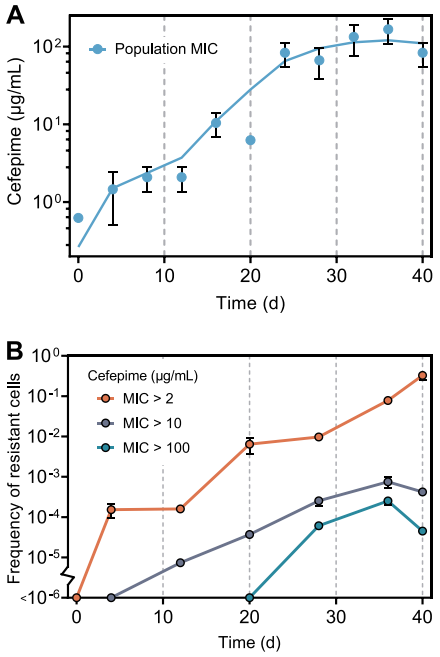

Figure 1. (A) Increases in the cefepime MIC of the *C. testosteroni* population during the 40 day experimental evolution when exposed to 10 ng/mL cefepime. The curve was smoothed by four neighbors to the average and 2nd order of the smoothing polynomial. (B) Frequencies of resistant cells with different levels of antibiotic resistance (cefepime MICs > 2, 10, and 100 μg/mL, respectively). Error bars indicate standard deviations from biological triplicates.

across replicated lineages (Figure S4, Table S2). Over 200-fold increases in population MICs were observed in antibiotic-exposed cultures, whereas the resistance level of the control groups without cefepime was unchanged during the 40 day subculture. Due to heteroresistance, i.e., the resistance of individual cells emerged earlier than that of the total population,[25] the detection of cells with MICs higher than the population MIC was expected throughout experimental evolution. Indeed, cells with an MIC > 2 μg/mL emerged as early as day 4 and continuously increased to 40% of the total population on day 40. The frequencies of cells with an MIC > 10 μg/mL also increased from 10^{-5} on day 12 to 10^{-4} on day 40. Highly resistant cells with an MIC > 100 μg/mL were detected starting from day 28 and represented 10^{-5} of the total population on day 40 (Figure 1B, Table S3). Despite the late appearance and extremely low frequency, the MICs of strongly resistant mutants were close to the ultimate MIC of the overall population.[10] It was confirmed that tolerance was not the survival strategy of the resistant subpopulations on day 40 in response to environmental concentrations of cefepime (Figure S5). As a result, it is essential to predict the emergence of high-

https://doi.org/10.1021/acs.est.2c00793
Environ. Sci. Technol. 2022, 56, 15074−15083

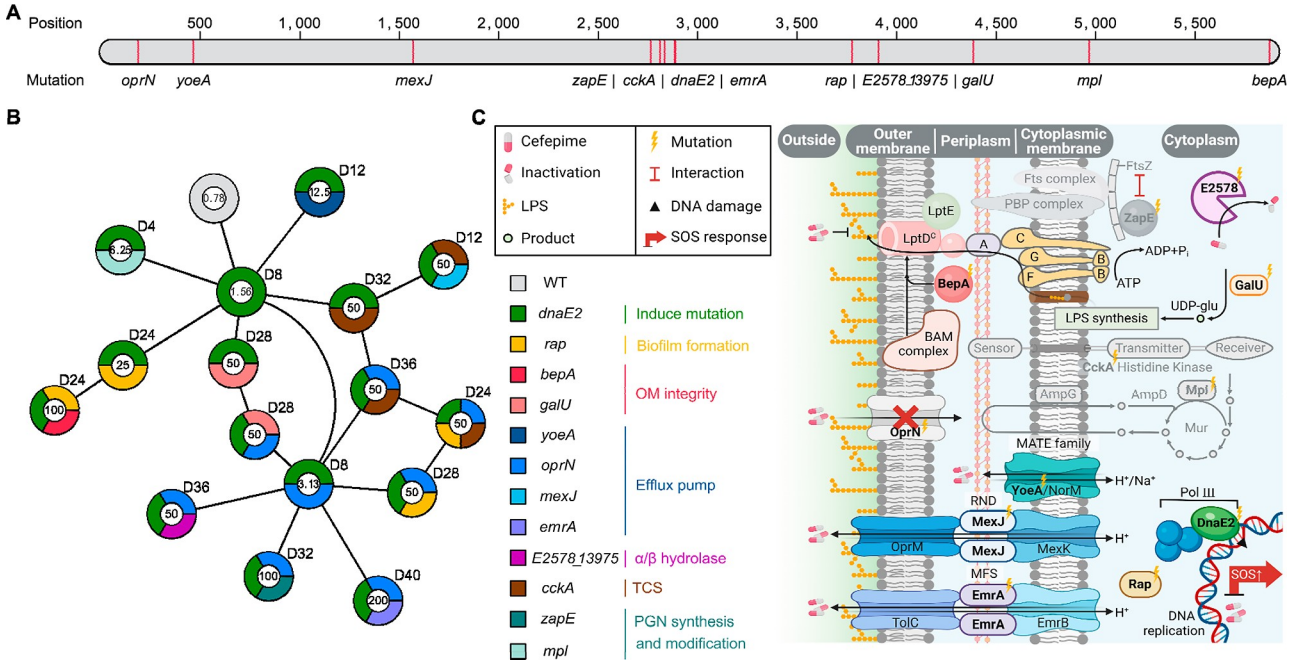

Figure 2. Evolutionary trajectory and molecular mechanism of cefepime resistance. (A) Mutations occurred in the genome of *C. testosteroni* during experimental evolution. Red bars indicate mutated genes. (B) Evolutionary trajectory of cefepime resistance. Hollow circles: resistant genotypes; filled colors: mutated genes; values in the center: cefepime MIC (in μg/mL); values in the upper right: isolation time of specific genotypes; edges: connections between genotypes with evolutionary relationships. Mutated genes are classified according to their functions. (C) Schematic view of the molecular mechanism involved in cefepime resistance evolution.

level resistant mutants in a population and estimate their resistance levels.

In addition to elevated phenotypic antibiotic resistance, we also observed: (1) growth inhibition [During the first 20 days of experimental evolution, the daily end point OD_{600} values were 0.8−1.0, significantly lower than that of the control group without cefepime (OD_{600} at around 1.2, Figure S6A).]; (2) increased biofilm formation. The biofilm formation potential of planktonic cells was uniformly low at the early stage of experimental evolution, which increased by up to three times on day 40 (Figure S6B). Similar growth inhibition occurred in the experimental evolution of *Escherichia coli* challenged with sub-MIC penicillin with approximately 25% OD_{600} reduction within the first day.[26] In another study on *Pseudomonas aeruginosa*, both planktonic and biofilm populations had increased biofilm formation potentials upon exposure to sub-MIC ciprofloxacin.[8] In Sections 3.2 and 3.3, mutations contributing to increased biofilm formation potential were identified and confirmed.

3.2. Evolutionary Trajectory and Mechanism of Cefepime Resistance. Resistance mutations, defined as nonsynonymous mutations causing over 2-fold increases in MICs, were broadly distributed in the genome of *C. testosteroni* (Figure 2A and Table S4). WGS analysis of the 60 mutants yielded 16 resistant genotypes, involving 12 mutated genes, conferring cefepime resistance at MICs of 1.56−200 μg/mL. The mutated genes included (grouped on the basis of function and emerged chronologically during experimental evolution): *dnaE2* (DNA replication), *rap* (biofilm formation), *bepA* and *galU* (OM integrity), *yoeA*, *oprN*, *mexJ*, and *emrA* (efflux pump), *E2578_13975* (α/β hydrolase), *cckA* (two-component system), and *zapE* and *mpl* (peptidoglycan synthesis and modification). The accumulation of three- or four-stepwise mutations could cause a hundred-fold increase in MICs. The highest resistance (MIC = 200 μg/mL) was found in a genotype with mutations in *dnaE2*, *oprN*, and *emrA*. Evolutionary trajectories of antibiotic resistance in the 16 genotypes were constructed on the basis of their mutations (Figure 2B). Cross-resistance was tested for nine evolved strains covering all mutated genes against seven representative antibiotics (Figure S7). Differences in the cross-resistance of nine genotypes were attributed to their different antimicrobial mechanisms. The evolution of resistance to azithromycin and cefepime was similar, while that for other antibiotics was associated with the genetic backgrounds of mutants. For example, the *zapE* and *mexJ* mutations conferred a high-level resistance to imipenem. The *mpl* mutation increased the susceptibility to ciprofloxacin and tobramycin. None of the evolved strains induced cross-resistance to ciprofloxacin.

The *dnaE2* (I1111 V) mutation existed in all 16 resistant genotypes. DnaE2 is an error-prone DNA polymerase relevant to DNA damage-induced mutagenesis.[27] A previous study has shown that DnaE2 was the primary mediator of *Mycobacterium tuberculosis* survival under UV irradiation through inducible mutagenesis.[28] Although *dnaE2* is not a reported ARG, its mutation could directly contribute to the emergence of drug resistance. Additionally, *dnaE2* is universally present in the genomes of environmental microbes[29,30] and human pathogens,[31] such as *Pseudomonas*, *Streptomyces*, and *Mycobacterium* spp. Therefore, it is speculated that the *dnaE2* mutation at an early stage of resistance evolution could be a general strategy employed by these bacteria for the promotion of genetic heterogeneity and development of antibiotic resistance.

Other mutated genes and their functions are shown in Figure 2C: (1) biofilm formation [The mutants carrying the *rap* (S5629R) mutation exhibited relatively high cefepime resistance (MIC > 25 μg/mL). The *rap* gene is involved in autoaggregation, one of the first steps in biofilm formation,[32]

https://doi.org/10.1021/acs.est.2c00793
Environ. Sci. Technol. 2022, 56, 15074−15083

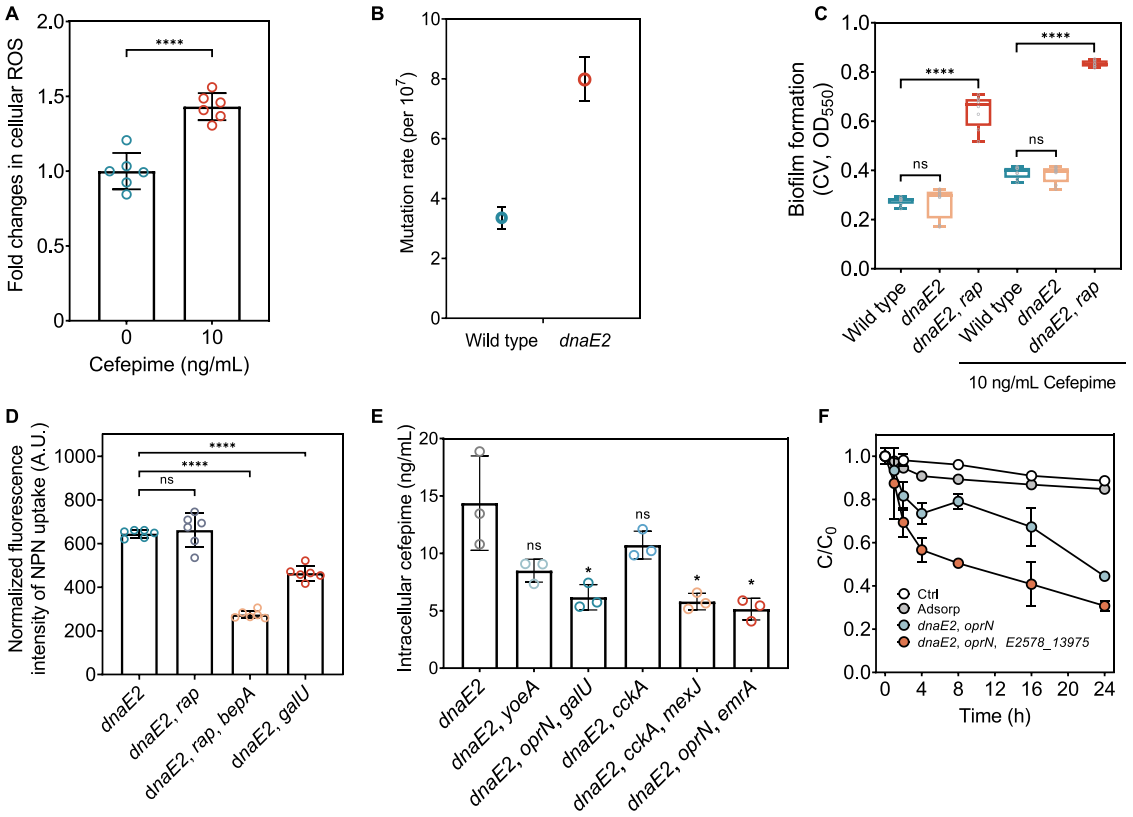

Figure 3. Validation of resistance-conferring mutations in *C. testosteroni* exposed to environmental concentrations of cefepime. (A) Fold changes in cellular ROS under the exposure of 10 ng/mL cefepime. (B) Mutation rates of the WT strain and *dnaE2* mutant based on fluctuation tests. (C) Biofilm formation potentials of the WT strain, *dnaE2* mutant, and *dnaE2+rap* double mutant determined by the crystal violet (CV) assay. (D) Outer membrane permeability determined by the NPN uptake assay. (E) Intracellular concentrations of cefepime in selected mutants after 30 min of exposure to cefepime at an initial concentration of 50 ng/mL. (F) Aerobic degradation of cefepime by two selected mutants. Initial concentration: 50 ng/mL. Control groups: without cells and with heat-inactivated cells. All experiments were conducted in at least three biological replicates. Significant differences between samples were indicated by asterisks (*: $p < 0.05$; ****: $p < 0.0001$; ns: not significant).

providing exposure protection to the cells by limiting cefepime diffusion into the population.];[2] (2) outer membrane integrity [Three highly resistant mutants (MIC = 50 μg/mL) carried mutations in *bepA* (A310 fs) and *galU* (G115_H116insLG), encoding proteins for the maintenance of OM integrity.[33,34] In particular, *galU* is involved in producing glycosyl donors for stress tolerance.];[35] (3) efflux pump [Multiple mutations involved in antibiotic efflux were detected in 10/16 genotypes, belonging to three different efflux pump protein families: *yoeA* (A534 fs) in the multidrug and toxic-compound extrusion (MATE) family, *oprN* (E273_I276del) and *mexJ* (Q107 fs) in the resistance-nodulation-division (RND) family, and *emrA* (R551 fs, P555 fs) in the major facilitator superfamily (MFS). These efflux pump systems are highly representative, allowing bacteria to survive in diverse environments under stress.[36] Remarkably, the mutant with the highest MIC (200 μg/mL) harbored the mutated *emrA*, suggesting its more important role in inducing high-level resistance compared with other efflux pump genes. Considering the fact that *emrA* is a frequently detected, clinically relevant ARG,[37] low-level cefepime exposure induced *emrA* mutation in environmental bacteria could emerge as a significant clinical problem.]; (4) antibiotic hydrolysis [Although the genome of *C. testosteroni* harbored genes encoding the beta-lactamase CTX enzyme, responsible for resistance to oxyimino-beta-lactam substrates (e.g., ceftazidime, ceftriaxone, or cefepime),[38] relevant mutations were not detected in this study. Instead, a mutation in *E2578_13975* (A59T), encoding α/β hydrolase that contains multiple active sites responsible for the degradation of aromatic compounds (e.g., biphenyl) was present in one mutant (MIC = 50 μg/mL).];[39] (5) two-component signaling (TCS) system [4/16 genotypes displayed mutations in *cckA* (Q328_L329insRNALETQ) encoding the TCS system.[40] Although the TCS system perceives and transduces small molecules (signals) in microorganisms to trigger cell division, metabolism, and antibiotic resistance, the exact mechanism remains ambiguous.];[41] (6) peptidoglycan (PGN) synthesis and modification [Mutations in *zapE* (E226 V) and *mpl* (L15R) pertaining to PGN synthesis and modification were found in 2/16 genotypes. ZapE is a conditional cell division protein,[42] but its role in conferring antibiotic resistance has not been reported. Mutations in *mpl* were frequently detected, displaying strong correlations with antibiotic resistance against ampicillin, ciprofloxacin, etc.[43] Nevertheless, its detailed antibiotic resistance mechanism is not yet known.]

3.3. Validated Roles of Mutations Conferring Cefepime Resistance. ROS significantly increased by 1.43-fold in the WT strain 10 min after cefepime exposure at 10 ng/mL (Figure 3A). ROS can damage DNA and disrupt cell division, leading to mutations.[44] Consequently, a representative subset of 16 isolated genotypes carrying individual or multiple mutations of *dnaE2*, *rap*, *bepA*, *galU*, *yoeA*, *oprN*, *mexJ*, *emrA*, and *E2578_13975* were chosen to validate the roles of key mutations conferring resistance evolution.

https://doi.org/10.1021/acs.est.2c00793
Environ. Sci. Technol. 2022, 56, 15074−15083

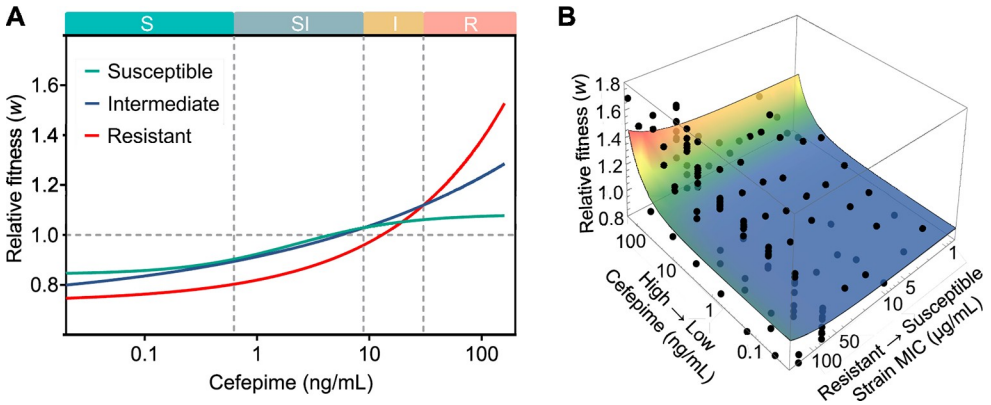

Figure 4. (A) Relative fitness of subpopulations exhibiting different levels of cefepime resistance. Subpopulations: susceptible (MIC < 16 μg/mL), intermediate (16 μg/mL < MIC < 64 μg/mL), and resistant (MIC > 64 μg/mL). Their relative fitness values were calculated at varied cefepime exposure concentrations, plotted, and fitted to the sigmoidal function (4PL). Selection windows for susceptible (S), susceptible−intermediate (SI), intermediate (I), and resistant (R) subpopulations were indicated on top of the graph. The relative fitness of the WT strain was set at 1 (horizontal dashed line, $w = 1$). (B) Relative fitness of 16 mutants at varied cefepime concentrations. All data points were fitted to the Gaussian nonlinear model ($n = 128$, $R^2 = 0.50$, p-value < 0.05).

The *dnaE2* mutation increased the bacterial mutation rate. On the basis of the Luria-Delbruck fluctuation test, the mutation rate of the *dnaE2* mutant was 2.38 times higher than that of the WT strain ($p < 0.05$, Figure 3B). Cefepime exposure induced this initial, key mutation of *dnaE2*, accelerating resistance evolution later on through diversified mutations, as has been demonstrated in *Mycobacterium tuberculosis*.[45]

The *rap* mutation promoted the biofilm formation. The biofilm formation potentials of the WT strain, *dnaE2* mutant, and *dnaE2* + *rap* double mutant were 0.28, 0.29, and 0.66, respectively (Figure 3C). The role of *rap* mutation, i.e., enhanced biofilm formation, was thus confirmed. Cefepime exposure at 10 ng/mL further increased the biofilm formation values, likely by stimulating *rap* expression.

The *bepA* and *galU* mutations reduced outer membrane permeability. The presence of *bepA* and *galU* mutation significantly reduced the fluorescence intensities of NPN uptake by 2.20- and 1.37-fold, respectively. The OM permeability was thus lower than those without the mutations (Figure 3D).

The *oprN*, *yoeA*, *mexJ*, and *emrA* mutations contributed to reduced cefepime uptake via downregulated expression of the porin channel and upregulated expressions of the efflux pumps. The intracellular cefepime concentrations measured 30 min after cefepime exposure at 50 ng/mL were lower in variants with these mutated genes, more specifically, by 41% with *yoeA*, 57% with *oprN*, 60% with *mexJ*, and 64% with *emrA*. Only 10% of the added cefepime was detected within the *emrA* mutant, which was in line with its highest resistance (MIC = 200 μg/mL) across all 16 mutants. In comparison, mutations in *yoeA* and *oprN* had limited contributions to decreased cefepime uptake, and thereby, the corresponding mutants had low MICs of 12.50 and 3.15 μg/mL, respectively (Figure 3E). Further, the mutated gene *oprN* was downregulated by 74−88% after the 3 h exposure to 1 μg/mL cefepime (Figure S8), and the decreased porin channel (OprN) activity likely hampered the diffusion of hydrophilic antibiotics.[46] The three efflux pump related genes *yoeA*, *mexJ*, and *emrA* had frameshift (fs) mutations, and were upregulated by 18.77-, 16.39-, and 4.48-fold. In general, indel mutations likely cause the loss of function and inhibit gene expression. However, some fs-mutated genes shared by cells were found to be not epigenetically silenced with potentials to be correctly expressed in the cells.[47]

The *E2578_13975* mutation led to upregulation of the gene encoding α/β hydrolase. In the adsorption group (cells were heat-inactivated), cefepime only decreased by <4% in 24 h, which was comparable to the control group (without cells). The *E2578_13975* variant degraded 69.21 ± 2.42% of the added 50 ng/mL cefepime within 24 h, while the degradation was only 55.54 ± 1.8% in the absence of the mutation (Figure 3F), and the differences in degradation efficiencies were significant ($p < 0.01$). This mutation caused the upregulation of α/β hydrolases by 38.17-fold (Figure S8), potentially inactivating antibiotics including but not limited to cefepime. Moreover, cefepime degradation products by α/β hydrolase and other enzymes, e.g., β-lactamase, were identified (Figures S9−S11, Table S5).[48] The resistance mechanism has a double-edged sword effect, as it decreases the antibiotic selection pressure to the surrounding sensitive species, alleviating AMR development in microbial communities.[2]

We propose five resistance mechanisms employed during resistance evolution: (i) the first key event was the *dnaE2* mutation, leading to an increase in the rate and diversity of cellular-level mutations; (ii) the enhanced biofilm formation promoted bacterial autoaggregation, providing exposure protection to the population; (iii) there was a reduction in outer membrane permeability and cefepime uptake; (iv) upregulated efflux pumps actively drained antibiotics from the cells; (v) cefepime was inactivated inside the cells.

3.4. Relative Fitness of Mutants and Cefepime Minimal Selective Concentration. The relative fitness of the 16 resistant genotypes was calculated on the basis of mono- and mixed-culture growth curve data.[23] The fitness of different resistant subpopulations was plotted (Figure 4A), and the cefepime selection windows for resistant (MIC > 64 μg/mL), intermediate (16 μg/mL < MIC < 64 μg/mL), and susceptible (MIC < 16 μg/mL) subpopulations were defined according to the CLSI's breakpoints, MIC values for other nonenterobacterales (Figure S12).[49] The susceptible, susceptible−intermediate, intermediate, and resistant subpopulations dominated in the concentration window #1 (0−0.6 ng/mL), #2 (0.6−8.5 ng/mL), #3 (8.5−30.7 ng/mL), and #4 (>30.7 ng/mL). Relative

https://doi.org/10.1021/acs.est.2c00793
Environ. Sci. Technol. 2022, 56, 15074−15083

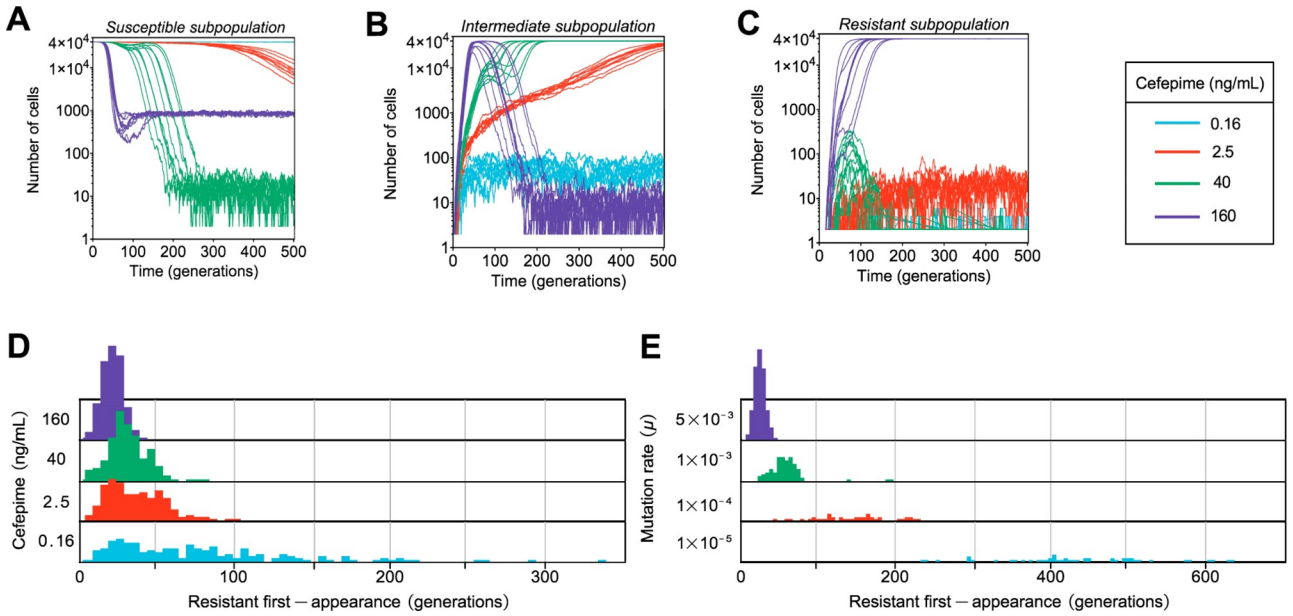

Figure 5. Agent-based model simulating population dynamics and resistance evolution at varied cefepime concentrations and mutation rates. Changes in the number of susceptible (A), intermediate (B), and resistant (C) subpopulations across 500 generations exposed corresponding to the four selective regions (S: 0.16 ng/mL; SI: 2.5 ng/mL; I: 40 ng/mL; R: 160 ng/mL, respectively). All simulations were repeated ten times (population size: $N = 40\,000$, $\mu = 5 \times 10^{-3}$). Histograms of the appearance time of resistant genotypes at different cefepime exposure concentrations (D) and mutation rates (E). The mutation rate was fixed at $\mu = 5 \times 10^{-3}$ in (D), and cefepime concentration was at 160 ng/mL in (E). All simulations were repeated 150 times.

fitness variations according to cefepime concentration, especially for the resistant subpopulation, exemplified a trade-off between resistance advantage and growth advantage. Gaussian nonlinear regression of the fitness data provided a more complete, three-dimensional view of the fitness−MIC−cefepime concentration correlations (Figure 4B).

Antibiotic concentrations between the minimal selective concentrations (MSCs) and the MIC of the WT strain lead to the enrichment of resistant bacteria.[50] MSCs typically fall within the range of 1/230 to 1/4 of the MIC_{WT} for different antibiotics.[51] Our results demonstrated that, for the susceptible subpopulation, the MSC value was 4.74 ± 0.15 ng/mL, 1/166 of the MIC_{WT}; the MSC for intermediate and resistant subpopulations were 5.76 ± 0.28 ng/mL (1/135 of the MIC_{WT}) and 13.61 ± 0.21 ng/mL (1/57 of the MIC_{WT}), respectively. Cefepime concentrations detected in antibiotic polluted environments, e.g., wastewater treatment plants, were sometimes higher than the MSC of resistant mutants,[18] rendering these places as hotspots of cefepime resistance.

3.5. Predictable Resistance Evolution under Varied Cefepime Selection Pressures and Mutation Rates. Agent-based modeling of the extended Moran process is a novel approach to simulate evolutionary dynamics of antibiotic resistance at varied antibiotic selection pressures and mutation rates. The conventional Moran process contained only two alleles, which was extended to include 17 genotypes with an interrelationship described by the evolutionary trajectory matrix. Simulations were performed as evolution games on a two-dimensional chessboard, where each grid represented one cell. All cells started with the WT genotype, and at each simulation step (one generation), they could jump forward or backward to the adjacent vertex (mutant genotype) in the evolutionary trajectories by a possibility factor equal to the mutation rate. The probabilities of mutation−selection were determined by the relative fitness of the mutants. The effectiveness of the modeling approach was tested by comparing the simulated and experimental resistance frequencies (Figure S13). The probability of mutation−selection was then determined by the relative fitness of the mutants using the *Curveball* package in Python.[23]

Population dynamics were simulated in 500 generations, where the environmental selection pressures were at 0.16, 2.5, 40, and 160 ng/mL (representing the concentration windows #1, #2, #3, and #4, respectively). Under relatively high cefepime selection pressures (40 and 160 ng/mL), the susceptible subpopulation lost their dominance within 100−200 generations (Figure 5A). The intermediate subpopulations dominated under the intermediate selection pressures (0.25 and 40 ng/mL) but were outcompeted by susceptible and resistant subpopulations under the weakest and strongest selection pressures (0.16 and 160 ng/mL), respectively (Figure 5B). The growth of the resistant subpopulation under high selection pressure (160 ng/mL) surpassed that of susceptible and intermediate subpopulations within 50−100 generations (Figure 5C). The estimated earliest emergence time of the resistant subpopulation was 10 generations (160 ng/mL), but even at low selection pressure (2.5 ng/mL), they emerged around 100 generations and resided in the population (Figure 5D). Statistically, the expected emergence time of the resistant subpopulations was negatively correlated with the selection pressure and mutation rate (Figure 5D,E). The rationale for setting the values (population size and mutation rate) is described in the Supporting Information Methods Section. More details of the simulated population dynamics are displayed in Figure S14A−D.

Under mild antibiotic selection, the evolutionary end point of resistance from a given starting point was usually not predetermined.[52] Instead of evolving adaptive outcomes (i.e., higher resistance), organisms can sometimes become "trapped" by their evolutionary responses to stresses (i.e., cefepime

https://doi.org/10.1021/acs.est.2c00793
Environ. Sci. Technol. 2022, 56, 15074−15083

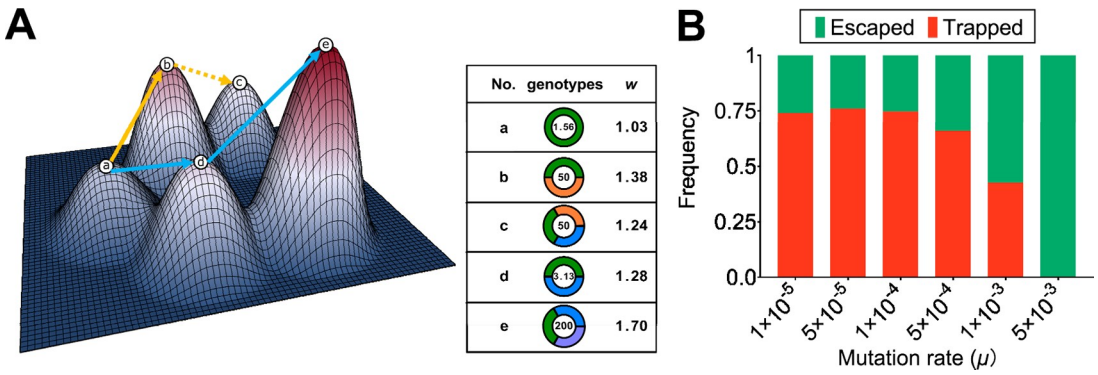

Figure 6. (A) Fitness landscape of the selected five resistant genotypes under cefepime exposure at 160 ng/mL. The *xy* plane represents genotype space, and the *z*-axis represents relative fitness. Starting from the susceptible genotype a, the blue arrow shows its evolutionary trajectory via susceptible genotype d to highly resistant genotype e (escaping the evolutionary trap). The orange arrow shows its evolutionary trajectory via genotype b to an intermediate genotype c (entering the evolutionary trap). (B) Frequencies of subpopulations escaping and entering the evolutionary trap b at varied mutation rates.

exposure) and experience reduced survival or reproduction. In this study, an evolutionary trap was found in the fitness landscape constructed under high selection pressure (160 ng/mL), and the "escaped" and "trapped" evolutionary pathways were depicted (Figure 6A). The escaped pathway led to the highly resistant genotype (e.g., peak e), whereas the trapped pathway resulted in stalling in the intermediate genotype (e.g., peak b). 150 repeated simulations consistently suggested that an increased mutation rate can dramatically increase the frequency of escaping evolutionary traps (Figures 6B and S15), reducing the evolution obstacles to high antibiotic resistance. On the basis of the simulated results, the emergence of highly resistant genotypes was assured at a mutation rate higher than 5×10^{-3}. Various environmental disturbances such as UV irradiation, toxicants, and low temperature can result in increased mutation rates.[53] Higher mutation rates would benefit the evolution of high-level antibiotic resistance as bacteria can escape evolutionary traps more frequently. Given the mutation rates of environmental microbes, agent-based modeling can predict their possibilities of escaping evolutionary traps and evolving highly resistant genotypes. It should be noted that the application of the agent-based Moran model in predicting real-world antibiotic resistance has certain limitations: (1) antibiotic concentrations are not constant, especially in real environments; (2) in response to antibiotic stresses, cells do not act independently, and their metabolite exchange and population protection would affect resistance evolution, which has not been considered in the current model.

3.6. Environmental Implications. Some of the resistance mechanisms revealed in this study (e.g., the initial mutation of *dnaE2* that increases the mutation rate) may be common strategies employed by numerous environmental microbes under the stresses of broader antibiotics at environmental concentrations. Environmental perturbations and oxidative stresses other than antibiotics likely lead to further increases in bacterial mutation rates that accelerate diversified evolution trajectories of antibiotic resistance.[54] As a result, more clinically relevant ARG mutations could be induced, such as *emrA*, contributing to the development of high-level antibiotic resistance from the environment to the clinic. The reduction of selective pressures of antibiotics and/or other oxidative stresses is effective in decreasing mutation rates and mitigating the development of antibiotic resistance.

Theoretically, the agent-based modeling approach can be applied to study the resistance evolution of any environmental microbe exposed to low-level antibiotics. It is capable of simulating population dynamics based on the mutation−selection process and predicting the emergence of highly resistant genotypes and their frequency in the population. Its applications to simulate the resistance evolution of bacterial communities in the real environment should also consider the effects of horizontal gene transfer, changes in community structure and function, and species competition for resources. Specifically, the lowest antibiotic concentration that can lead to antibiotic resistance development (i.e., predicted MSC) could serve as a reference for regulatory standards of antibiotics in the environment. The above results are of significance in the enrichment of the current knowledge on antibiotic resistance arising in the environment and guiding global practices toward antibiotic resistance control.

■ ASSOCIATED CONTENT

Supporting Information

The Supporting Information is available free of charge at https://pubs.acs.org/doi/10.1021/acs.est.2c00793.

Additional methods, detailed information on phenotypic characterizations, bioinformatic analysis, the measurement of cefepime and the identification of its degradation products, and model parameter settings (PDF)

Accession Codes

All WGS data have been deposited in the NCBI BioProject under accession no. PRJNA794302. The ABM code is available from the corresponding author upon request.

■ AUTHOR INFORMATION

Corresponding Authors

Huijie Lu − *College of Environmental and Resource Sciences and Academy of Ecological Civilization, Zhejiang University, Hangzhou, Zhejiang 310058, China;* orcid.org/0000-0002-0076-4508; Email: luhuijie@zju.edu.cn

Youjun Feng − *Departments of Microbiology & General Intensive Care Unit of the Second Affiliated Hospital, Zhejiang University School of Medicine, Hangzhou, Zhejiang 310058, China;* orcid.org/0000-0001-8083-0175; Email: fengyj@zju.edu.cn

https://doi.org/10.1021/acs.est.2c00793
Environ. Sci. Technol. 2022, 56, 15074−15083

Author

Hanqing Wang − *College of Environmental and Resource Sciences, Zhejiang University, Hangzhou, Zhejiang 310058, China*

Complete contact information is available at: https://pubs.acs.org/10.1021/acs.est.2c00793

Notes

The authors declare no competing financial interest.

■ ACKNOWLEDGMENTS

The authors would like to thank the "Major Program of National Natural Science Foundation of China (Grant No. 22193061)" and the "Fundamental Research Funds for the Central Universities (Grant No. 2021QNA6007)" for their financial support. We are grateful to Dr. Xichang Zhang from Zhejiang University for the technical support.

■ REFERENCES

(1) Hsueh, P.-R. World Health Day 2011−Antimicrobial Resistance: No Action Today, No Cure Tomorrow. *J. Formos. Med. Assoc.* **2011**, *110* (4), 213−214.

(2) Bottery, M. J.; Pitchford, J. W.; Friman, V.-P. Ecology and Evolution of Antimicrobial Resistance in Bacterial Communities. *Isme J.* **2021**, *15* (4), 939−948.

(3) Gullberg, E.; Cao, S.; Berg, O. G.; Ilbäck, C.; Sandegren, L.; Hughes, D.; Andersson, D. I. Selection of Resistant Bacteria at Very Low Antibiotic Concentrations. *Plos Pathog.* **2011**, *7* (7), No. e1002158.

(4) Loos, R.; Marinov, D.; Sanseverino, I.; Napierska, D.; Lettieri, T. *Review of the 1st Watch List under the Water Framework Directive and Recommendations for the 2nd Watch List*; EUR 29173 EN; European Commission, 2018; DOI: 10.2760/614367.

(5) Vikesland, P. J.; Pruden, A.; Alvarez, P. J. J.; Aga, D.; Bürgmann, H.; Li, X.; Manaia, C. M.; Nambi, I.; Wigginton, K.; Zhang, T.; Zhu, Y.-G. Toward a Comprehensive Strategy to Mitigate Dissemination of Environmental Sources of Antibiotic Resistance. *Environ. Sci. Technol.* **2017**, *51* (22), 13061−13069.

(6) Jørgensen, K. M.; Wassermann, T.; Jensen, P. Ø.; Hengzuang, W.; Molin, S.; Høiby, N.; Ciofu, O. Sublethal Ciprofloxacin Treatment Leads to Rapid Development of High-Level Ciprofloxacin Resistance during Long-Term Experimental Evolution of *Pseudomonas aeruginosa*. *Antimicrob. Agents Ch.* **2013**, *57* (9), 4215−4221.

(7) Wistrand-Yuen, E.; Knopp, M.; Hjort, K.; Koskiniemi, S.; Berg, O. G.; Andersson, D. I. Evolution of High-Level Resistance during Low-Level Antibiotic Exposure. *Nat. Commun.* **2018**, *9* (1), 1599.

(8) Santos-Lopez, A.; Marshall, C. W.; Scribner, M. R.; Snyder, D. J.; Cooper, V. S. Evolutionary Pathways to Antibiotic Resistance Are Dependent upon Environmental Structure and Bacterial Lifestyle. *Elife* **2019**, *8*, No. e47612.

(9) Marcusson, L. L.; Frimodt-Møller, N.; Hughes, D. Interplay in the Selection of Fluoroquinolone Resistance and Bacterial Fitness. *Plos Pathog.* **2009**, *5* (8), No. e1000541.

(10) Xing, Y.; Kang, X.; Zhang, S.; Men, Y. Specific Phenotypic, Genomic, and Fitness Evolutionary Trajectories toward Streptomycin Resistance Induced by Pesticide Co-Stressors in *Escherichia coli*. *Isme Commun.* **2021**, *1* (1), 39.

(11) Ma, Y.-F.; Zhang, Y.; Zhang, J.-Y.; Chen, D.-W.; Zhu, Y.; Zheng, H.; Wang, S.-Y.; Jiang, C.-Y.; Zhao, G.-P.; Liu, S.-J. The Complete Genome of *Comamonas testosteroni* Reveals Its Genetic Adaptations to Changing Environments▽ †. *Appl. Environ. Microb.* **2009**, *75* (21), 6812−6819.

(12) Phale, P. S.; Malhotra, H.; Shah, B. A. Degradation Strategies and Associated Regulatory Mechanisms/Features for Aromatic Compound Metabolism in Bacteria. *Adv. Appl. Microbiol.* **2020**, *112*, 1−65.

(13) Ji, Q.; Zhang, C.; Li, D. Influences and Mechanisms of Nanofullerene on the Horizontal Transfer of Plasmid-Encoded Antibiotic Resistance Genes between *E. coli* Strains. *Front. Env. Sci. Eng.* **2020**, *14* (6), 108.

(14) Vardanyan, R.; Hruby, V. Antibiotics. In *Synthesis of Best-Seller Drugs*; Academic Press, 2016; pp 573−643;.

(15) Kohanski, M. A.; Dwyer, D. J.; Collins, J. J. How Antibiotics Kill Bacteria: From Targets to Networks. *Nat. Rev. Microbiol.* **2010**, *8* (6), 423−435.

(16) Rosenkilde, C. E. H.; Munck, C.; Porse, A.; Linkevicius, M.; Andersson, D. I.; Sommer, M. O. A. Collateral Sensitivity Constrains Resistance Evolution of the CTX-M-15 β-Lactamase. *Nat. Commun.* **2019**, *10* (1), 618.

(17) Weinreich, D. M.; Delaney, N. F.; DePristo, M. A.; Hartl, D. L. Darwinian Evolution Can Follow Only Very Few Mutational Paths to Fitter Proteins. *Science* **2006**, *312* (5770), 111−114.

(18) Yao, S.; Ye, J.; Yang, Q.; Hu, Y.; Zhang, T.; Jiang, L.; Munezero, S.; Lin, K.; Cui, C. Occurrence and Removal of Antibiotics, Antibiotic Resistance Genes, and Bacterial Communities in Hospital Wastewater. *Environ. Sci. Pollut. R.* **2021**, *28* (40), 57321−57333.

(19) Bridges, B. A. The Fluctuation Test. *Arch. Toxicol.* **1980**, *46* (1−2), 41−44.

(20) Papkou, A.; Hedge, J.; Kapel, N.; Young, B.; MacLean, R. C. Efflux Pump Activity Potentiates the Evolution of Antibiotic Resistance across *S. aureus Isolates*. *Nat. Commun.* **2020**, *11* (1), 3970.

(21) Hoben, H. J.; Somasegaran, P. Comparison of the Pour, Spread, and Drop Plate Methods for Enumeration of *Rhizobium* spp. in Inoculants Made from Presterilized Peat. *Appl. Environ. Microb.* **1982**, *44* (5), 1246−1247.

(22) Hall, B. M.; Ma, C.-X.; Liang, P.; Singh, K. K. Fluctuation AnaLysis CalculatOR: A Web Tool for the Determination of Mutation Rate Using Luria−Delbrück Fluctuation Analysis. *Bioinformatics* **2009**, *25* (12), 1564−1565.

(23) Ram, Y.; Dellus-Gur, E.; Bibi, M.; Karkare, K.; Obolski, U.; Feldman, M. W.; Cooper, T. F.; Berman, J.; Hadany, L. Predicting Microbial Growth in a Mixed Culture from Growth Curve Data. *Proc. National Acad. Sci.* **2019**, *116* (29), 14698−14707.

(24) Lieberman, E.; Hauert, C.; Nowak, M. A. Evolutionary Dynamics on Graphs. *Nature* **2005**, *433* (7023), 312−316.

(25) Nicoloff, H.; Hjort, K.; Levin, B. R.; Andersson, D. I. The High Prevalence of Antibiotic Heteroresistance in Pathogenic Bacteria Is Mainly Caused by Gene Amplification. *Nat. Microbiol.* **2019**, *4* (3), 504−514.

(26) Lopatkin, A. J.; Bening, S. C.; Manson, A. L.; Stokes, J. M.; Kohanski, M. A.; Badran, A. H.; Earl, A. M.; Cheney, N. J.; Yang, J. H.; Collins, J. J. Clinically Relevant Mutations in Core Metabolic Genes Confer Antibiotic Resistance. *Science* **2021**, *371* (6531), eaba0862.

(27) Peng, R.; Chen, J.; Feng, W.; Zhang, Z.; Yin, J.; Li, Z.; Li, Y. Error-Prone DnaE2 Balances the Genome Mutation Rates in *Myxococcus xanthus* DK1622. *Front. Microbiol.* **2017**, *8*, 122.

(28) Boshoff, H. I. M.; Reed, M. B.; Barry, C. E.; Mizrahi, V. DnaE2 Polymerase Contributes to In Vivo Survival and the Emergence of Drug Resistance in *Mycobacterium tuberculosis*. *Cell* **2003**, *113* (2), 183−193.

(29) Koorits, L.; Tegova, R.; Tark, M.; Tarassova, K.; Tover, A.; Kivisaar, M. Study of Involvement of ImuB and DnaE2 in Stationary-Phase Mutagenesis in *Pseudomonas putida*. *Dna Repair* **2007**, *6* (6), 863−868.

(30) Tsai, H.-H.; Shu, H.-W.; Yang, C.-C.; Chen, C. W. Translesion-Synthesis DNA Polymerases Participate in Replication of the Telomeres in *Streptomyces*. *Nucleic Acids Res.* **2012**, *40* (3), 1118−1130.

(31) Friedberg, E. C.; Fischhaber, P. L. TB or Not TB How *Mycobacterium tuberculosis* May Evade Drug Treatment. *Cell* **2003**, *113* (2), 139−140.

(32) Trunk, T.; Khalil, H. S.; Leo, J. C. Bacterial Autoaggregation. *AIMS Microbiol.* **2018**, *4* (1), 140−164.

(33) Okuda, S.; Sherman, D. J.; Silhavy, T. J.; Ruiz, N.; Kahne, D. Lipopolysaccharide Transport and Assembly at the Outer Membrane: The PEZ Model. *Nat. Rev. Microbiol.* **2016**, *14* (6), 337−345.
(34) Haeusser, D. P.; Margolin, W. Splitsville: Structural and Functional Insights into the Dynamic Bacterial Z Ring. *Nat. Rev. Microbiol.* **2016**, *14* (5), 305−319.
(35) Liao, C.-T.; Du, S.-C.; Lo, H.-H.; Hsiao, Y.-M. The GalU Gene of *Xanthomonas campestris* Pv. Campestris Is Involved in Bacterial Attachment, Cell Motility, Polysaccharide Synthesis, Virulence, and Tolerance to Various Stresses. *Arch. Microbiol.* **2014**, *196* (10), 729−738.
(36) Piddock, L. J. V. Multidrug-Resistance Efflux Pumps - Not Just for Resistance. *Nat. Rev. Microbiol.* **2006**, *4* (8), 629−636.
(37) Zhang, A.-N.; Gaston, J. M.; Dai, C. L.; Zhao, S.; Poyet, M.; Groussin, M.; Yin, X.; Li, L.-G.; van Loosdrecht, M. C. M.; Topp, E.; Gillings, M. R.; Hanage, W. P.; Tiedje, J. M.; Moniz, K.; Alm, E. J.; Zhang, T. An Omics-Based Framework for Assessing the Health Risk of Antimicrobial Resistance Genes. *Nat. Commun.* **2021**, *12* (1), 4765.
(38) Porse, A.; Jahn, L. J.; Ellabaan, M. M. H.; Sommer, M. O. A. Dominant Resistance and Negative Epistasis Can Limit the Co-Selection of de Novo Resistance Mutations and Antibiotic Resistance Genes. *Nat. Commun.* **2020**, *11* (1), 1199.
(39) Li, C.; Li, J.-J.; Montgomery, M. G.; Wood, S. P.; Bugg, T. D. H. Catalytic Role for Arginine 188 in the C−C Hydrolase Catalytic Mechanism for *Escherichia coli* MhpC and *Burkholderia xenovorans* LB400 BphD †. *Biochemistry-us* **2006**, *45* (41), 12470−12479.
(40) Jacobs, C.; Domian, I. J.; Maddock, J. R.; Shapiro, L. Cell Cycle−Dependent Polar Localization of an Essential Bacterial Histidine Kinase That Controls DNA Replication and Cell Division. *Cell* **1999**, *97* (1), 111−120.
(41) Jacob-Dubuisson, F.; Mechaly, A.; Betton, J.-M.; Antoine, R. Structural Insights into the Signalling Mechanisms of Two-Component Systems. *Nat. Rev. Microbiol.* **2018**, *16* (10), 585−593.
(42) Egan, A. J. F.; Errington, J.; Vollmer, W. Regulation of Peptidoglycan Synthesis and Remodelling. *Nat. Rev. Microbiol.* **2020**, *18* (8), 446−460.
(43) Li, Y.; Xia, L.; Chen, J.; Lian, Y.; Dandekar, A. A.; Xu, F.; Wang, M. Resistance Elicited by Sub-Lethal Concentrations of Ampicillin Is Partially Mediated by Quorum Sensing in *Pseudomonas aeruginosa*. *Environ. Int.* **2021**, *156*, 106619.
(44) Boles, B. R.; Singh, P. K. Endogenous Oxidative Stress Produces Diversity and Adaptability in Biofilm Communities. *Proc. National Acad. Sci.* **2008**, *105* (34), 12503−12508.
(45) Ford, C. B.; Shah, R. R.; Maeda, M. K.; Gagneux, S.; Murray, M. B.; Cohen, T.; Johnston, J. C.; Gardy, J.; Lipsitch, M.; Fortune, S. M. *Mycobacterium tuberculosis* Mutation Rate Estimates from Different Lineages Predict Substantial Differences in the Emergence of Drug-Resistant Tuberculosis. *Nat. Genet.* **2013**, *45* (7), 784−790.
(46) Delcour, A. H. Outer Membrane Permeability and Antibiotic Resistance. *Biochimica. Et. Biophysica. Acta. Bba. - Proteins Proteom.* **2009**, *1794* (5), 808−816.
(47) Roudko, V.; Bozkus, C. C.; Orfanelli, T.; McClain, C. B.; Carr, C.; O'Donnell, T.; Chakraborty, L.; Samstein, R.; Huang, K.; Blank, S. V.; Greenbaum, B.; Bhardwaj, N. Shared Immunogenic Poly-Epitope Frameshift Mutations in Microsatellite Unstable Tumors. *Cell* **2020**, *183* (6), 1634−1649.E17.
(48) Yau, M.-H.; Wang, J.; Tsang, P. W. K.; Fong, W.-P. J1 Acylase, a Glutaryl-7-aminocephalosporanic Acid Acylase from *Bacillus laterosporus* J1, Is a Member of the α/B-hydrolase Fold Superfamily. *Febs. Lett.* **2006**, *580* (5), 1465−1471.
(49) CLSI. *Performance Standards for Antimicrobial Susceptibility Testing*, 31st ed.; CLSI, 2021.
(50) Kraupner, N.; Ebmeyer, S.; Bengtsson-Palme, J.; Fick, J.; Kristiansson, E.; Flach, C.-F.; Larsson, D. G. J. Selective Concentration for Ciprofloxacin Resistance in *Escherichia coli* Grown in Complex Aquatic Bacterial Biofilms. *Environ. Int.* **2018**, *116*, 255−268.
(51) Gullberg, E.; Albrecht, L. M.; Karlsson, C.; Sandegren, L.; Andersson, D. I. Selection of a Multidrug Resistance Plasmid by Sublethal Levels of Antibiotics and Heavy Metals. *Mbio* **2014**, *5* (5), e01918−14.
(52) Steinberg, B.; Ostermeier, M. Environmental Changes Bridge Evolutionary Valleys. *Sci. Adv.* **2016**, *2* (1), No. e1500921.
(53) Björkholm, B.; Sjölund, M.; Falk, P. G.; Berg, O. G.; Engstrand, L.; Andersson, D. I. Mutation Frequency and Biological Cost of Antibiotic Resistance in *Helicobacter pylori*. *Proc. National Acad. Sci.* **2001**, *98* (25), 14607−14612.
(54) Wang, Y.; Lu, J.; Engelstädter, J.; Zhang, S.; Ding, P.; Mao, L.; Yuan, Z.; Bond, P. L.; Guo, J. Non-Antibiotic Pharmaceuticals Enhance the Transmission of Exogenous Antibiotic Resistance Genes through Bacterial Transformation. *Isme J.* **2020**, *14* (8), 2179−2196.

https://doi.org/10.1021/acs.est.2c00793
Environ. Sci. Technol. 2022, 56, 15074−15083